



# HHS Public Access

Author manuscript

Nat Med. Author manuscript; available in PMC 2012 September 01.

Published in final edited form as:

Nat Med. ; 18(3): 463–467. doi:10.1038/nm.2666.

## Self-Assembling Nanocomplexes by combining Ferumoxytol, Heparin And Protamine For Cell Tracking by MRI

Mya S. Thu<sup>1</sup>, L. Henry Bryant<sup>1</sup>, Tiziana Coppola<sup>1</sup>, E. Kay Jordan<sup>1</sup>, Matthew D. Budde<sup>1</sup>, Bobbi K. Lewis<sup>1</sup>, Aneeka Chaudhry<sup>1</sup>, Jiaqiang Ren<sup>2</sup>, Nadimpalli Ravi S. Varma<sup>3</sup>, Ali S. Arbab<sup>3</sup>, and Joseph A. Frank<sup>1,4</sup>

<sup>1</sup>Frank Laboratory and Laboratory of Diagnostic Radiology Research, Department of Radiology and Imaging Sciences, National Institutes of Health, Bethesda, MD, U.S.A.

<sup>2</sup>Cell Processing Section, Department of Transfusion Medicine, Clinical Center, National Institutes of Health, Bethesda, MD, U.S.A.

<sup>3</sup>Cellular and Molecular Imaging Laboratory, Department of Radiology, Henry Ford Hospital, Detroit, MI, U.S.A.

<sup>4</sup>National Institute of Biomedical Imaging and Bioengineering, National Institutes of Health, Bethesda, MD, U.S.A

### Abstract

We report on a novel and straightforward magnetic cell labeling approach that combines three FDA-approved drugs, ferumoxytol (F), heparin (H) and protamine (P) in serum free media to form self-assembling nanocomplexes that effectively label cells for *in vivo* MRI. We observed that the HPF nanocomplexes were stable in serum free cell culture media. HPF nanocomplexes exhibited a three-fold increase in T2 relaxivity compared to F. Electron Microscopy revealed internalized HPF within endosomes, confirmed by Prussian blue staining of labeled cells. There was no long-term effect or toxicity on cellular physiology or function of HPF-labeled hematopoietic stem cells, bone marrow stromal cells, neural stem cells, and T-cells when compared to controls. *In vivo* MRI detected 1000 HPF-labeled cells implanted in rat brains. HPF labeling method should facilitate the monitoring by MRI of infused or implanted cells in clinical trials.

### Keywords

ferumoxytol; protamine sulfate; heparin sulfate; ultrasmall superparamagnetic iron oxide nanoparticles; self assembly; stem cells; cell labeling; MRI

---

Users may view, print, copy, download and text and data- mine the content in such documents, for the purposes of academic research, subject always to the full Conditions of use: [http://www.nature.com/authors/editorial\\_policies/license.html#terms](http://www.nature.com/authors/editorial_policies/license.html#terms)

Corresponding Author: Joseph A Frank, MS MD, Building 10 Room B1N256, 10 Center Dr MSC 1074, Bethesda, Maryland 20892, Phone: 301-402-4314, Fax: 301-402-3216, [j frank@helix.nih.gov](mailto:j frank@helix.nih.gov).

### AUTHOR CONTRIBUTIONS

Guarantors of integrity of entire study, JAF, MST, LHB; Study concepts/design, JAF, MST; Data acquisition, MST, LHB, EKJ, BKL, AC, MDB, NRSV, JR, ASA; Data analysis/interpretation, JAF, MST, LHB, EKJ, JR, ASA; Manuscript drafting or manuscript revision for important intellectual content, JAF, MST, LHB; Manuscript final approval, all authors; Statistical analysis, MST; Manuscript editing, JAF, MST.

## INTRODUCTION

Cell-based therapies have become a major focus in regenerative medicine and tumor trials<sup>1-3</sup>. To understand the effects of cellular therapies, non-invasive imaging approaches have been developed that would allow for the monitoring of the migration of cell products<sup>4</sup>. Presently, cell trafficking studies in the clinic depend on either radiolabeling of cells or the addition of reporter genes into the cell genome coupled with a radionuclide or positron-emitting probe for imaging, most of which require approval by the Food and Drug Administration (FDA)<sup>4-6</sup>. Short half-life of isotopes, renal toxicity, leakage of the radioactive label or insertion of viral particles in random tissues are possible limitations of these approaches<sup>4, 5</sup>. Magnetic Resonance Imaging (MRI) coupled with magnetically labeled cells provides excellent alternative to track cells because of its inherent soft-tissue contrast, high spatial resolution and lack of ionizing radiation<sup>4, 7</sup>.

Clinically approved superparamagnetic iron oxide nanoparticles (SPION) are used for the treatment of iron deficiency anemia<sup>8-11</sup>, or have been used as contrast agents to detect pathology<sup>7, 12, 13</sup> or to visualize transplanted cells<sup>7</sup>. SPION are usually carbohydrate dextran-coated and are biodegradable<sup>14</sup>. Various methods<sup>15-21</sup> have been developed to label cells with SPION providing the ability to monitor transplanted cells by MRI. In order to facilitate the translation of MR tracking as part of the cellular therapy, techniques were developed combining clinical grade SPION, ferumoxides (FE) with protamine (P) to label cells without short or long-term toxicity or alteration in their functional capacity or stemness<sup>16, 22, 23</sup>. However, ferumoxides and similar SPION were removed from the market thus, halting the progress towards translating this approach to label and track cells by MRI for clinical trials.

Recently, ferumoxytol (F), a semi-synthetic carbohydrate non-dextran-coated ultrasmall SPION (USPIO), has been approved for the treatment of iron deficiency anemia in chronic kidney disease<sup>8-11, 13</sup>. Ferumoxytol has been used in experimental and clinical trials as a macrophage imaging agent as well as blood pool agent with MRI<sup>13, 24</sup>. Ferumoxytol alone or in combination with protamine does not effectively label cells<sup>10, 11, 13</sup>.

The purpose of this study is to report on a novel and straightforward approach using three FDA-approved drugs (albeit off-label), ferumoxytol, heparin (H) and protamine to label cells for MRI that has potential implications for cell-based therapy. Heparin is an anticoagulant and protamine is used to reverse heparin anticoagulation effects. H and P form nanocomplexes *in vitro* and *in vivo* through electrostatic interactions<sup>25</sup> and have been used to facilitate intracellular drug delivery<sup>26, 27</sup>. Combining heparin, protamine and ferumoxytol results in the formation of a self-assembling nanocomplex (HPF) that was characterized and used to label stem cells or immune cells for MRI. Labeling cells with HPF was nontoxic to cells and therefore should facilitate the rapid translation of this technique to clinical trials.

## RESULTS

### Chemical characterization of HPF nanocomplexes

The chemical characteristics of heparin<sup>28</sup>, protamine<sup>25–29</sup>, ferumoxylol<sup>9–11, 13, 24</sup> and various combinations of the agents are as follows; the HPF nanocomplexes at the ratio of H (2 IU ml<sup>-1</sup>): P (60 µg ml<sup>-1</sup>): F (50 µg ml<sup>-1</sup>) used to magnetically label cells had a zeta potential (ζ) of 14.1 ± 3.43 mV and size of 204 nm in water, and a ζ of -10.9 ± 0.0 and size of 153.6 nm in RPMI at 37 °C (Fig. 1a and Supplementary Table 1). Transmission Electron Microscopy (TEM) micrographs of the HPF nanocomplexes reveal F as electron dense iron nanoparticles coating the clear HP aggregates in an ovoid shape, of approximately 150–200 nm in diameter (Fig. 1b, c).

### Cell labeling and iron content

Approximately 100% of the HPF-labeled cells were Prussian blue (PB) or PB-DAB positive on histology (Fig. 2a–j). The internalization of HPF in endosomes was confirmed by TEM (Fig. 3) with HPF appearing as electron dense iron oxide nanoparticles that are approximately 6–8 nm in size. HPF was not observed on the cell membrane following cell washes. To determine the longevity of intracellular iron, NSC, BMSC and T-cells were labeled with HPF, and were either allowed to proliferate and divided or were grown to confluence and exhibited contact inhibition. Labeled cells were stained at multiple time points to determine the presence of intracellular iron (Supplementary Figs. 1 and 2). PB positive T-cells, NSC or BMSC could be detected for 7 or 14 days when repeatedly cultured, whereas PB-DAB positive were detected for 21 days (NSC) and 28 days (BMSC) when grown to confluence.

The average iron content per cell was as follows: BMSC = 2.12 ± 0.11 picograms (pg); NSC = 2.8 ± 1.19 pg; HSC = 1.33 ± 0.2 pg; T-cells = 0.73 ± 0.25 pg; and Monocytes = 2.56 ± 1.1 pg. The iron content of unlabeled cells contained 0.0–0.5 pg cell<sup>-1</sup> which was significantly different from labeled cells (p < 0.05). We were unable to label cells with ferumoxylol alone or when combined with protamine over a wide range of ratios.

### HPF cells: toxicity, phenotype, differentiation and function

There were no substantial differences in the rate of apoptosis, increases in reactive oxygen species (ROS), viability or proliferation 1–4 days following labeling with HPF for all cell types as compared to controls (Fig. 4). A slight decrease was observed in numbers of NSC (6%) and T-cells (10%) immediately after cell collection (Fig. 4a) and in proliferation of NSC and HSC at days 3–4 compared to control cells (Fig. 4b). The proliferative capacity recovered overtime when the cells were assessed at Day 7 for NSC and Day 30 for HSC. Phenotypic analyses of HPF-labeled and unlabeled BMSC surface markers were positive for surface markers CD90, CD73, CD105 (Supplementary Fig. 3). In this study, HPF-labeled BMSCs were cryo-preserved and subsequently thawed for analysis. These results revealed that there were no effects on cellular viability (Supplementary Fig. 3a) or surface markers (Supplementary Fig. 3b–d) after freeze-thaw cycle, indicating that it is not necessary to immediately label cells prior to use. The differentiation potential of HPF-labeled BMSCs towards adipogenic and osteogenic lineages demonstrated no differences when compared to

controls (Supplementary Fig. 4). There were no differences in chemotactic migration towards tumor-conditioned media or SDF-1 $\alpha$  when comparing HPF-labeled BMSC or NSC to unlabeled controls (Supplementary Fig. 5).

### ***In Vivo* MRI**

*In vivo* MR images obtained at clinically relevant field strength of 3 Tesla of a rat brain with intra-cerebral implantation of HPF-labeled BMSCs revealed hypointense voxels at the injection sites that received  $10^3$  to  $10^4$  labeled BMSCs compared to surrounding parenchyma or unlabeled cells (Fig. 5). Implanted HPF-labeled cells were detected because of T2 and T2\* shortening (Fig. 5a). Calculated T2\* maps at Day 8 demonstrated a substantial (30–60%) decrease in T2\* values for the  $10^3$ – $10^4$  labeled cells (T2\* = 30.9–34.3 ms) compared to surrounding brain (T2\* = 67.5 ms) and unlabeled cells (T2\* = 48.0 ms) (Fig. 5b). HPF-labeled BMSCs implanted at  $10^3$  and  $5 \times 10^3$  appear to have shorter T2\* values (32.9 ms and 30.9 ms respectively) compared to that of  $10^4$  HPF-labeled cells (34.3 ms) (Fig. 5b). This lack of correlation between the number of HPF-labeled BMSC and T2\* change at the injection site of  $10^4$  HPF-labeled cells was possibly due to the volumetric effect at the MRI slice (i.e., 500 $\mu$ m) shown or unequal distribution of the density of HPF-labeled cells at the injection site. Moreover, the quantification of the numbers of labeled cells from R2\* measurements is inexact especially when monitoring cells overtime due to hemorrhage, dead cells, cell density and iron load, or susceptibility effects between tissue<sup>4, 30</sup>. Photomicrographs of the area of the brain implanted with  $10^3$  HPF-labeled BMSC demonstrated co-localization of anti-human Mitochondrial antibody stains with multiple PB-DAB positive human BMSC (Fig. 5c, d).

## **DISCUSSION**

The major finding of this study is the formation of self-assembling HPF nanocomplexes by simply combining three FDA approved drugs, ferumoxytol, heparin and protamine directly into media containing cells, resulting in the labeling of stem cells and immune cells for cellular tracking and detection by MRI. Combining P with F results in the formation of large, polydisperse complexes that were not incorporated into cells. Neuwelt *et al.*<sup>13</sup> reported that PF complexes were unable to label rat blood mononuclear cells. Although it is counterintuitive to add heparin to PF to facilitate endosomal incorporation in cells, the addition of heparin gives rise to the formation of HPF nanocomplexes that were endocytosed by cells. Heparin-based nanoparticles self-assemble with a variety of cationic molecules and have been used for drug delivery, tissue engineering or for prolonging circulating half-life of an agent<sup>26, 28, 31</sup>. When heparin and protamine are mixed together, they rapidly form complexes through electrostatic interactions<sup>25, 26, 29</sup>. We observed that in RPMI, HP complexes form and then attracts F resulting in stable HPF nanocomplexes. Mixing HPF in an alternative order such as FHP also results in nanocomplexes that can be used for cell labeling; however, other combinations of the drugs (i.e., P:F:H) did not label cells. TEM of HP aggregates coated with colloidal iron demonstrated a dense ring of iron around a HP hypodense center<sup>29</sup>, similar to HPF nanocomplexes. Further investigation is required to elucidate the ultrastructure and chemical composition of the HPF nanocomplexes in order to achieve effective iron loading of cells while preserving cell viability and function.

Heparin, protamine and ferumoxytol are routinely used for specific clinical indications. The concentrations of H, P and F used in this study results in intracellular concentrations of each drug that were substantially below recommended clinical doses. The HPF nanocomplexes have similar biochemical properties to SPION that have been shown to label cells and biodegrade through iron metabolic pathway<sup>16, 22, 23, 32</sup>. We have also demonstrated that HPF-labeled NSC and BMSC remained PB positive for up to 28 days similar to observations in stem cells labeled with SPION<sup>16, 32</sup>. Although further investigation is needed to determine any potential toxicity of delivering HPF-labeled cells *in vivo*, ferumoxytol is likely to be metabolized similar to other SPIONs. As with previous findings of SPION-labeled cells, dilution of the endosomal HPF nanocomplexes will likely occur through cell division or via digestion<sup>33, 34</sup>.

In this study, we were able to clearly visualize as few as 1000 cells at 8 days post intracerebral transplantation on T2\* weighted images due to T2\* shortening and the susceptibility blooming artifact associated with the HPF-labeled cells at 3 Tesla. The intracellular location of HPF nanocomplexes results in T2\* shortening of water protons by causing magnetic field gradients in the region of interest. Hemorrhage at the site of injection may also cause T2\* shortening and represents a limitation of interpreting MRI cell tracking studies of SPION labeled cells<sup>4, 14, 16</sup>. Although the labeled cell death will occur overtime, we previously reported that approximately 10–20% of the iron label in transplanted cells maybe endocytosed by activated macrophages but minimally contributed to hypointense voxels on MRI<sup>35</sup>. The T2\* weighted images employed in this study allowed for short acquisition times (approximately 10 minutes) without modification to the clinical MR scanner. Although the intracellular concentration of iron of HPF-labeled stem cells was less than cells labeled with SPION, the iron content is comparable to reports in which cells were labeled with other USPIO nanoparticles<sup>15, 18, 21, 36</sup>. The intracellular iron content is dependent on the cell surface area and nuclear to cytoplasmic ratio with larger cells having the potential to uptake greater amounts of SPION<sup>4, 16</sup>.

With the removal of the clinically available SPION contrast agents from the market, cell therapy trials that planned to incorporate magnetic cell labeling to monitor the cell migration were placed on hold or abandoned. Ferumoxytol is the only intravenous FDA-approved USPIO nanoparticle preparation that could be used to magnetically label and monitor the temporal spatial migration of infused or implanted cells by MRI. One of the major advantages of complexing ferumoxytol with heparin and protamine to label cells was that they were clinically used, therefore, extensive safety testing of the drugs should not be necessary and the time required for evaluating HPF for an investigative new drug application shortened. Although standard operating procedure protocols will need to be developed, the HPF labeling method presented in this study allows for the easy scale-up for cell labeling in current good manufacturing practice cell processing facility. Further optimization of the HPF protocol by modifying the amount of heparin (i.e., 1–3 IU ml<sup>-1</sup>), protamine (i.e., 30 – 60 µg ml<sup>-1</sup>) or increasing the amount of ferumoxytol (i.e., 50–100 µg ml<sup>-1</sup>) may result in higher intracellular iron concentrations, providing the basis for the rapid translation into clinical trials.

## METHODS

### HPF nanocomplex preparation

Ferumoxytol (Feraheme®, AMAG Pharmaceuticals, Inc.) contains particle size of 17–31 nm in diameter with the 6 nm iron oxide crystals core with a polyglucose sorbitol carboxymethylether coating. The stock preparation of Feraheme has an iron content of 30 mg ml<sup>-1</sup> and contains mannitol at 44 mg ml<sup>-1</sup><sup>9</sup>. Heparin sulfate (1000 IU ml<sup>-1</sup>) and protamine sulfate (10 mg ml<sup>-1</sup>) (both from American Pharmaceuticals Partner, LLC) were used to form HPF nanocomplexes. The HPF complexes were prepared by sequentially adding H at 2 IU ml<sup>-1</sup>, P at 60 µg ml<sup>-1</sup> and F at 50 µg ml<sup>-1</sup> in either sterile water for physiochemical characterization or in serum free RPMI-1640 media for cell culture studies. The three drugs were also mixed as FHP in the same ratio for effective labeling of HSCs.

### Cell labeling

All adherent monolayer cells were grown to 80–90 % confluence and cells in suspension were spun down and re-suspended in 4×10<sup>6</sup> cells ml<sup>-1</sup> for labeling. BMSC, monocytes, T-cells and HSC were labeled in serum-free RPMI-1640 and NSCs were labeled in serum-free DMEM. For T-cells, 10 ng ml<sup>-1</sup> interleukin 2 (Peprotech) was supplemented for continuous stimulation of T-cells. The cells were labeled according to the following procedures: for each cell type, H (2 IU ml<sup>-1</sup>), P (60 µg ml<sup>-1</sup>) and F (50 µg ml<sup>-1</sup>) were added from stock drugs using appropriate serum-free media to cells in culture and incubated for 2–4 hours. Following incubation in serum free media, an equal amount of complete media containing 10–20% Fetal Bovine Serum (FBS) was then added and the cells were incubated overnight for each cell type. Cells were washed with Phosphate-Buffered Saline (PBS) (Invitrogen), or Hanks' Balanced Salt Solution (HBSS) (Invitrogen) followed by washes with 10 U ml<sup>-1</sup> Heparin to remove the residual HPF. TrypLE Express was used for detachment of BMSC and 0.25% trypsin-EDTA (both Invitrogen) was used for NSC.

### MRI of labeled cells

In order to determine the sensitivity of MRI at 3 Tesla to HPF-labeled cells *in vivo*, NIH RNU<sup>-/-</sup> rats (n= 6) (Charles Rivers Laboratories) underwent stereo-tactically guided intracranial injections of HPF-labeled and unlabeled BMSC at various cell concentrations in 5 µl sterile PBS at 4 sites in each brain. The numbers of HPF-labeled or unlabeled BMSCs implanted ranged from 10<sup>3</sup>–10<sup>4</sup> cells. MRI was performed on a clinical 3 T unit (Achieva, Philips Medical System) using a 4 cm solenoid coil (Philips Research Laboratories). MRI was performed with T2-weighted (T2w) turbo spin echo, repetition time (T<sub>R</sub>)/echo time (T<sub>E</sub>) = 3600/9.2 and 60 ms, T2\* multi echo multi Fast Field Echo (FFE), T<sub>R</sub> = 6200 ms, 15 echos with effective T<sub>E</sub> at 4.8 ms, flip angle 30°; and T2\*w FFE 3D sequence at T<sub>R</sub>/T<sub>E</sub> = 50–559.3/15–30 ms, flip angle 30°. All images were collected with field of view of 50 mm, slice thickness 500 µm with a final in-plane resolution of 100 × 100 µm. Scans were performed 1 and 8 days following implantation of labeled or unlabeled cells in the rat brains. T2\* maps were fit to a single exponential decay using Medx software (Medical Numerics). All experimental studies were performed to the approved Animal Care and Use Committee at the Clinical Center, National Institutes of Health.

## Histology

Following incubation with HPF, cells were fixed and Prussian blue (PB) staining or immunohistochemistry or immunofluorescence was performed. PB staining protocol was used as previously described to detect iron-positive HPF-labeled cells<sup>16, 19</sup>. For diaminobenzide (DAB)-enhanced PB, cytopins were put into hydrogen peroxide-activated DAB solution for < 10 minutes, washed with PBS, and counterstained with nuclear fast red. Labeling efficiency was performed by light microscopy on cells that were either PB or DAB enhanced positive for intracellular iron nanoparticles, expressed as a percentage of positive cells per five high power fields. For histopathology, rats were perfused with heparinized PBS and 4% paraformaldehyde + 3% sucrose solution. Brains were then harvested and cryopreserved for immunohistochemistry analysis. For detection of HPF-labeled BMSC or NSC in the rat brain with primary mouse IgG1 monoclonal antihuman Mitochondrial antibody (huMito) (ab3298, Abcam), immunofluorescent staining was performed on 10  $\mu$ m thick frozen sections. Microscopy studies were performed using Zeiss Axio Imager microscope (AxioPlan Imaging II, Carl Zeiss) using AxioVision software 4.7. Confocal microscopy (Axio LSM 710, Carl Zeiss) was performed for the huMito staining on frozen 10 $\mu$ m thick sections.

## Statistical analysis

Statistical analysis was performed using two-tailed student t-test. GraphPad Prism version 5.0 or spreadsheet software was used to determine significance. All data were shown as mean  $\pm$  standard deviation. Each experiment was performed in triplicate. P values <0.05 was considered statistically significant.

## Supplementary Material

Refer to Web version on PubMed Central for supplementary material.

## Acknowledgments

This work was supported and performed in part in the intramural research program in the Clinical Center at the US National Institutes of Health (NIH). Bone Marrow Stromal Cells were provided from the Center for Bone Marrow Stromal Cell Transplantation at the NIH. Neural Stem Cells were provided as part of a material transfer agreement with Karen. Aboody, City of Hope Medical Center, Duarte, CA. The authors would like to acknowledge the Clinical Image Processing Section at the NIH. This work was also supported by a grant from the NIH R01CA122031.

## References

1. Daley GQ. Prospects for stem cell therapeutics: myths and medicines. *Curr Opin Genet Dev.* 2002; 12:607–613. [PubMed: 12200167]
2. Mooney DJ, Vandenburgh H. Cell delivery mechanisms for tissue repair. *Cell Stem Cell.* 2008; 2:205–213. [PubMed: 18371446]
3. Motaln H, Schichor C, Lah TT. Human mesenchymal stem cells and their use in cell-based therapies. *Cancer.* 2010; 116:2519–2530. [PubMed: 20301117]
4. Arbab AS, et al. *In Vivo* Cellular Imaging for Translational Medical Research. *Curr Med Imaging Rev.* 2009; 5:19–38. [PubMed: 19768136]
5. Modo M. Noninvasive imaging of transplanted cells. *Curr Opin Organ Transplant.* 2008; 13:654–658. [PubMed: 19060558]

6. Yaghoubi SS, Gambhir SS. PET imaging of herpes simplex virus type 1 thymidine kinase (HSV1-tk) or mutant HSV1-sr39tk reporter gene expression in mice and humans using [<sup>18</sup>F]FHBG. *Nat Protoc.* 2006; 1:3069–3075. [PubMed: 17406570]
7. Bulte JW. *In vivo* MRI cell tracking: clinical studies. *AJR Am J Roentgenol.* 2009; 193:314–325. [PubMed: 19620426]
8. Schwenk MH. Ferumoxytol: a new intravenous iron preparation for the treatment of iron deficiency anemia in patients with chronic kidney disease. *Pharmacotherapy.* 2010; 30:70–79. [PubMed: 20030475]
9. Ferumoxytol (Feraheme) - a new parenteral iron formulation. *Med Lett Drugs Ther.* 2010; 52:23.
10. Auerbach M. Ferumoxytol as a new, safer, easier-to-administer intravenous iron: yes or no? *Am J Kidney Dis.* 2008; 52:826–829. [PubMed: 18971010]
11. Provenzano R, et al. Ferumoxytol as an intravenous iron replacement therapy in hemodialysis patients. *Clin J Am Soc Nephrol.* 2009; 4:386–393. [PubMed: 19176796]
12. Santoro L, et al. Resovist enhanced MR imaging of the liver: does quantitative assessment help in focal lesion classification and characterization? *J Magn Reson Imaging.* 2009; 30:1012–1020. [PubMed: 19856433]
13. Neuwelt EA, et al. Ultrasmall superparamagnetic iron oxides (USPIOs): a future alternative magnetic resonance (MR) contrast agent for patients at risk for nephrogenic systemic fibrosis (NSF)? *Kidney Int.* 2009; 75:465–474. [PubMed: 18843256]
14. Corot C, Robert P, Idee JM, Port M. Recent advances in iron oxide nanocrystal technology for medical imaging. *Adv Drug Deliv Rev.* 2006; 58:1471–1504. [PubMed: 17116343]
15. Boutry S, et al. Magnetic labeling of non-phagocytic adherent cells with iron oxide nanoparticles: a comprehensive study. *Contrast Media Mol Imaging.* 2008; 3:223–232. [PubMed: 19072771]
16. Arbab AS, et al. Efficient magnetic cell labeling with protamine sulfate complexed to ferumoxides for cellular MRI. *Blood.* 2004; 104:1217–1223. [PubMed: 15100158]
17. Arbab AS, et al. Comparison of transfection agents in forming complexes with ferumoxides, cell labeling efficiency, and cellular viability. *Mol Imaging.* 2004; 3:24–32. [PubMed: 15142409]
18. Golovko DM, et al. Accelerated stem cell labeling with ferucarbotran and protamine. *Eur Radiol.* 2010; 20:640–648. [PubMed: 19756632]
19. Walczak P, Kedziorek DA, Gilad AA, Lin S, Bulte JW. Instant MR labeling of stem cells using magnetoelectroporation. *Magn Reson Med.* 2005; 54:769–774. [PubMed: 16161115]
20. Xie D, et al. Optimization of magnetosonoporation for stem cell labeling. *NMR Biomed.* 2010; 23:480–484. [PubMed: 20213856]
21. Josephson L, Tung CH, Moore A, Weissleder R. High-efficiency intracellular magnetic labeling with novel superparamagnetic-Tat peptide conjugates. *Bioconjug Chem.* 1999; 10:186–191. [PubMed: 10077466]
22. Janic B, et al. Optimization and validation of FePro cell labeling method. *PLoS One.* 2009; 4:e5873. [PubMed: 19517015]
23. Balakumaran A, et al. Superparamagnetic iron oxide nanoparticles labeling of bone marrow stromal (mesenchymal) cells does not affect their “stemness”. *PLoS One.* 2010; 5:e11462. [PubMed: 20628641]
24. Neuwelt EA, et al. The potential of ferumoxytol nanoparticle magnetic resonance imaging, perfusion, and angiography in central nervous system malignancy: a pilot study. *Neurosurgery.* 2007; 60:601–611. discussion 611–602. [PubMed: 17415196]
25. Aborg CH, Uvnas B. Mode of binding of histamine and some other biogenic amines to a protamine-heparin complex *in vitro*. *Acta Physiol Scand.* 1968; 74:552–567. [PubMed: 5735618]
26. Liang JF, Song H, Li YT, Yang VC. A novel heparin/protamine-based pro-drug type delivery system for protease drugs. *J Pharm Sci.* 2000; 89:664–673. [PubMed: 10756332]
27. Liang JF, et al. ATTEMPTS: a heparin/protamine-based delivery system for enzyme drugs. *J Control Release.* 2002; 78:67–79. [PubMed: 11772450]
28. Kemp MM, Linhardt RJ. Heparin-based nanoparticles. *Wiley Interdiscip Rev Nanomed Nanobiotechnol.* 2010; 2:77–87. [PubMed: 20049832]

29. Rossmann P, Matousovic K, Horacek V. Protamine-heparin aggregates. Their fine structure, histochemistry, and renal deposition. *Virchows Arch B Cell Pathol Incl Mol Pathol*. 1982; 40:81–98. [PubMed: 6126957]
30. Liu W, Frank JA. Detection and Quantification of Magnetically Labeled Cells by Cellular MRI. *European Journal of Radiology*. 2009; 70:258–64. [PubMed: 18995978]
31. Khurshid H. Development of heparin-coated nanoparticles for targeted drug delivery applications. *J of Applied Physics*. 2009; 105:07B308.
32. Pawelczyk E, Arbab AS, Pandit S, Hu E, Frank JA. Expression of transferrin receptor and ferritin following ferumoxides-protamine sulfate labeling of cells: implications for cellular magnetic resonance imaging. *NMR Biomed*. 2006; 19:581–592. [PubMed: 16673357]
33. Arbab AS, et al. A model of lysosomal metabolism of dextran coated superparamagnetic iron oxide (SPIO) nanoparticles: implications for cellular magnetic resonance imaging. *NMR Biomed*. 2005; 18:383–389. [PubMed: 16013087]
34. Walczak P, Kedziorek DA, Gilad AA, Barnett BP, Bulte JW. Applicability and limitations of MR tracking of neural stem cells with asymmetric cell division and rapid turnover: the case of the shiverer dysmyelinated mouse brain. *Magn Reson Med*. 2007; 58:261–269. [PubMed: 17654572]
35. Pawelczyk E, et al. In Vivo Uptake of Intracellular Label by Tissue Macrophages from Prelabeled Bone Marrow Stromal Cells: Quantitative Analysis and Implications for Cellular Therapy. *PLoS ONE*. 2009; 4:e6712. [PubMed: 19696933]
36. Oude Engberink RD, van der Pol SM, Dopp EA, de Vries HE, Blezer EL. Comparison of SPIO and USPIO for *in vitro* labeling of human monocytes: MR detection and cell function. *Radiology*. 2007; 243:467–474. [PubMed: 17456871]
37. Rad AM, Janic B, Iskander AS, Soltanian-Zadeh H, Arbab AS. Measurement of quantity of iron in magnetically labeled cells: comparison among different UV/VIS spectrometric methods. *Biotechniques*. 2007; 43:627–628. 630, 632. passim. [PubMed: 18072592]

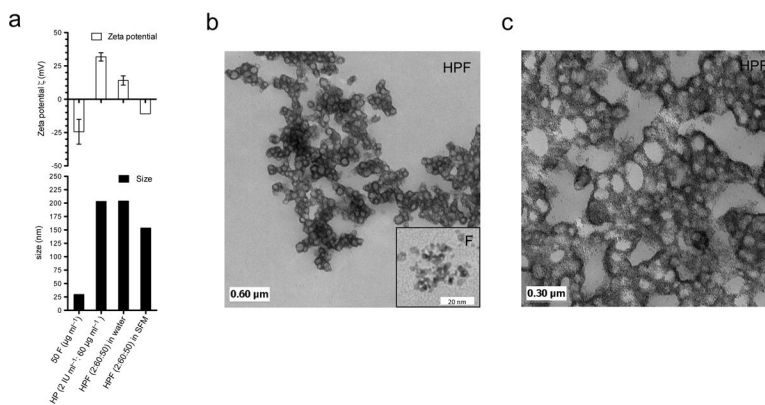


**Figure 1. Characteristics of self-assembling heparin (H), protamine (P), and ferumoxylol (F) nanocomplexes**  
**(a)** Graphs of the zeta potential ( $\zeta$ ) (top, white bar) and the particle size (bottom, black bar) of HPF nanocomplexes at  $2 \text{ IU ml}^{-1} \text{ H} : 60 \text{ } \mu\text{g ml}^{-1} \text{ P} : 50 \text{ } \mu\text{g ml}^{-1} \text{ F}$  in sterile water and serum free media; **(b)** HPF nanocomplexes formed by combining  $2 \text{ IU ml}^{-1} \text{ H} : 60 \text{ } \mu\text{g ml}^{-1} \text{ P} : 50 \text{ } \mu\text{g ml}^{-1} \text{ F}$  in sterile water and as observed by Transmission Electron Microscopy (TEM) with an inset showing native F nanoparticles; and **(c)** HPF at higher magnification. Scale bars:  $0.6 \text{ } \mu\text{m}$  (white thick bar, b),  $0.3 \text{ } \mu\text{m}$  (white thick bar, c) and  $20 \text{ nm}$  (white thick bar, b inset). Abbreviations: SFM: Serum Free Media

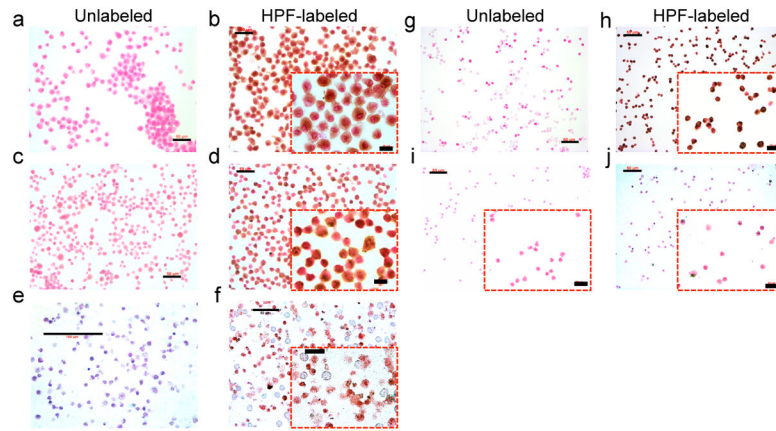


**Figure 2. Representative light microscopy images of DAB-enhanced Prussian blue (PB)-stained HPF-labeled human stem or immune cells**

(a) unlabeled bone marrow- stromal cells (BMSC), (b) PB-DAB enhanced HPF-labeled BMSC, (c) unlabeled neural stem cells (NSC), (d) PB-DAB enhanced HPF-labeled NSC, (e) unlabeled hematopoietic stem cells (HSC), (f) PB-DAB enhanced HPF-labeled HSC, (g) unlabeled monocytes, (h) PB-DAB enhanced HPF-labeled Monocytes, (i) Unlabeled T-cells, and (j) PB-DAB enhanced HPF-labeled T-cells. Scale bars: 100  $\mu\text{m}$  (black thin bar, e), 50  $\mu\text{m}$  (black thin bar, a–d and f–j) and 20  $\mu\text{m}$  (black thick bar, all dotted red boxes). Abbreviations: DAB: 3,3-diaminobenzidine.

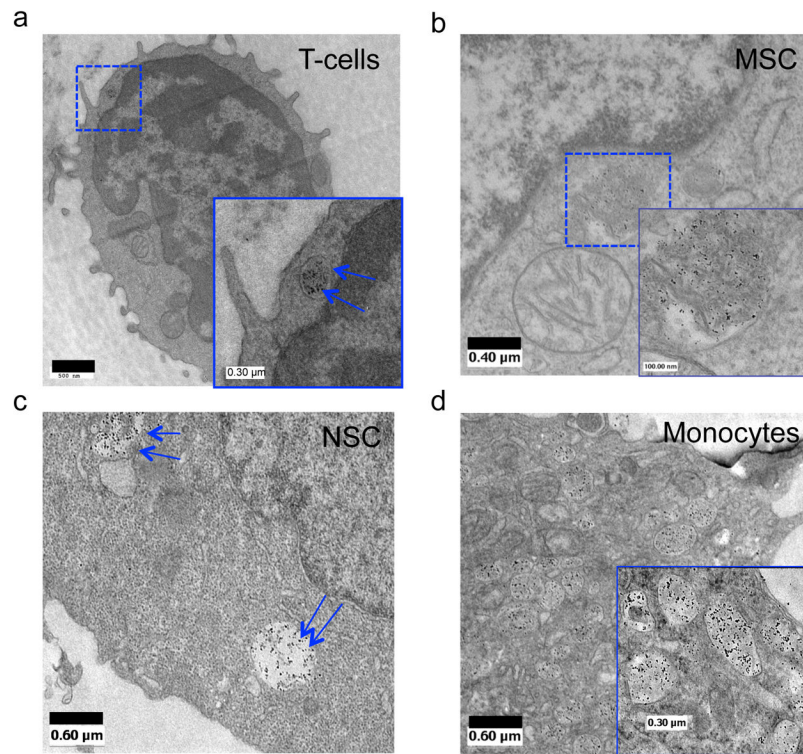


**Figure 3. Internalization and encapsulation of HPF nanocomplexes in HPF-labeled cells**  
 Transmission Electron Microscopy of (a) HPF-labeled T-cells, (b) HPF-labeled BMSC, (c) HPF-labeled NSC and (d) HPF-labeled Monocytes demonstrating that HPF nanocomplexes were encapsulated within the endosomes as electron dense nanoparticles (Blue arrows, a and c; and Blue dotted line and Blue inset, a, b and d). Scale bars: 0.6  $\mu\text{m}$  (black thick bar, c and d), 0.5  $\mu\text{m}$  (black thick bar, a), 0.4  $\mu\text{m}$  (black thick bar, b), 0.3  $\mu\text{m}$  (white thick bar, a and d insets) and 100 nm (white thick bar, b inset).

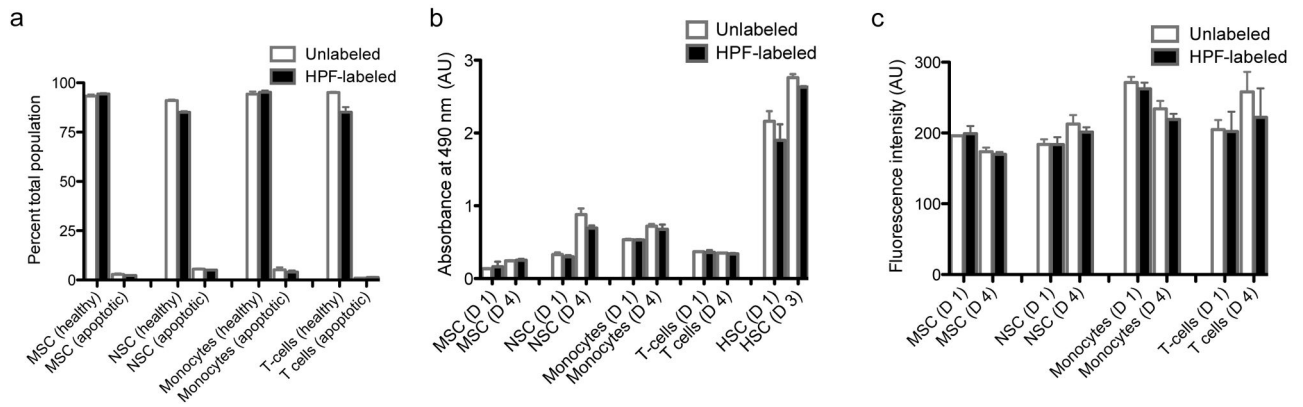


**Figure 4. Cellular physiological activity in HPF-labeled stem or immune cells**

(a) Rate of apoptosis immediately after cell collection post HPF labeling indicated by healthy and apoptotic population in unlabeled and HPF-labeled BMSC, NSC, HSC, Monocytes and T-cells. (b) Results of MTS proliferation assay of HPF-labeled cells at Day 1 (D 1) and Day 4 (D 4) compared to unlabeled control. (c) Results of reactive oxidative species (ROS) production in HPF-labeled cells at D 1 and D 4 as compared to unlabeled cells.

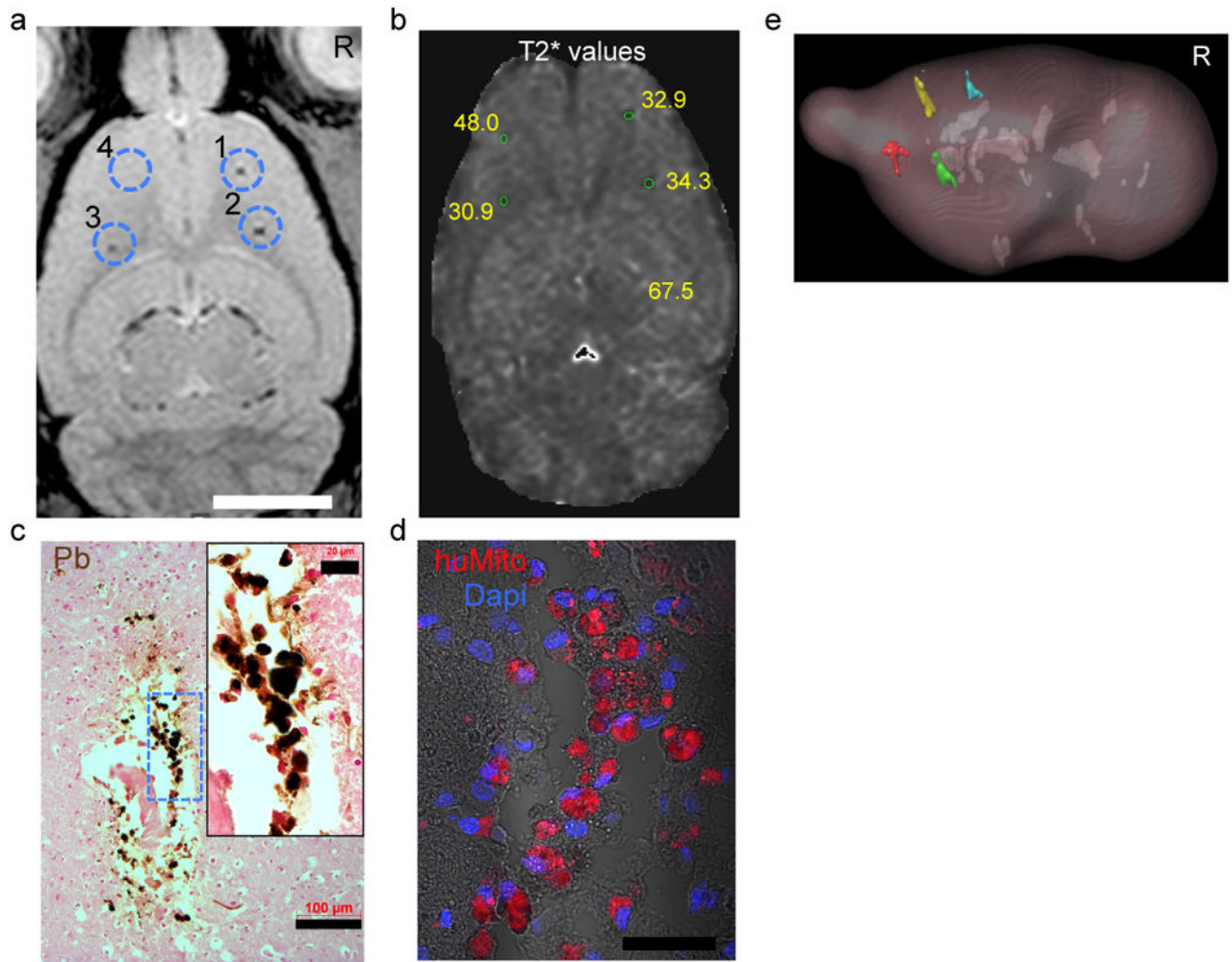


**Figure 5. *In vivo* MR visualization of intra-cranially-implanted HPF-labeled human BMSC in the rodent brain at 3T**

(a) *in vivo* MRI at 3T of HPF-labeled BMSC at the following locations with each location representing the injected cells: (1)  $10^3$  HPF-labeled BMSC, (2)  $10^4$  HPF-labeled BMSC, (3)  $5 \times 10^3$  HPF-labeled BMSC and (4)  $10^4$  unlabeled BMSC, (b) Calculated T2\* map with T2\* values at each injection site approximately corresponding to the MR slice in (a), (c) PB-DAB enhanced micrograph of the injection site that received  $10^3$  HPF-labeled BMSC, (d) Confocal image of anti-human Mitochondrial (huMito) antibody immunofluorescence staining of a consecutive tissue section in (c), (e) Three-dimensional rendering of the implanted cells within the rat brain in relation to the ventricles (white) can clearly be appreciated (Red =  $10^4$  unlabeled BMSC, Green =  $5 \times 10^3$  HPF-labeled BMSC, Yellow =  $10^3$  HPF-labeled BMSC and Cyan =  $10^4$  HPF-labeled BMSC. Scale bars: 0.5 cm (white thin bar, a), 100  $\mu$ m (black thin bar, c) and 20  $\mu$ m (black thick bar, c inset). Abbreviations: DAB: 3,3-diaminobenzidine.